Lateral Tunneling, Ballistic Transport, and Spectroscopy in a Two-Dimensional Electron Gas

A. Palevski, M. Heiblum, C. P. Umbach, C. M. Knoedler, A. N. Broers,[a] and R. H. Koch
IBM Research Division, T. J. Watson Research Center, Yorktown Heights, New York 10598
(Received 7 November 1988)

We report a direct observation, via electron energy spectroscopy, of lateral tunneling and lateral ballistic electron transport in a two-dimensional electron gas (2D EG). This was accomplished through the use of a novel transistor structure employing two potential barriers, induced by 50-nm-wide metal gates deposited on a GaAs/AlGaAs selectively doped heterostructure. Hot electrons with very narrow energy distributions ($\simeq$5 meV wide) have been observed to ballistically traverse 2D EG regions $\simeq$170 nm wide with a mean free path of about 480 nm.

PACS numbers: 73.40.Gk, 73.20.Dx

Ballistic transport of hot electrons was established recently in n^+-type GaAs by the use of energy spectroscopy in a hot-electron structure.[1] These experiments utilized an injector at one end of a transport region and a spectrometer at the other end, with the electrons moving normal to the plane of the layers (vertical transport). This technique proved to be very powerful since it permitted the energy distribution and the mean free path of the ballistic electrons to be determined. The very recent demonstration of quantized resistance in a confined quasi-two-dimensional electron gas (2D EG)[2,3] strongly suggests ballistic transport of electrons near equilibrium parallel to the interface between the layers (lateral transport). We report here the first utilization of an energy spectroscopy technique to establish *directly* lateral tunneling through an induced potential barrier and the existence of lateral ballistic transport in a 2D EG. This was done by inducing two closely spaced potential barriers in the 2D EG via two narrow Schottky metal gates deposited on the surface of the structure. One barrier was employed as a tunnel injector and the second as a spectrometer. We have measured narrow hot-electron distributions ballistically traversing lateral 2D EG regions 170 nm wide, and have estimated their mean free path.

Several structures were made on a selectively doped GaAs/AlGaAs heterostructure grown by molecular-beam epitaxy. On top of an undoped GaAs buffer layer, an undoped AlGaAs layer (50 nm thick, AlAs mole fraction $x=34\%$) was grown, followed by a thin heavily doped GaAs cap layer (15 nm thick). A sheet of Si atoms, with an areal density of $\simeq 2\times10^{12}$ cm^{-2}, was deposited under overpressure of As when growth of the AlGaAs was interrupted (planar doping), 30 nm away from the GaAs buffer layer; these supply the electrons in the 2D EG [Fig. 1(a)]. The 2D EG had a carrier density of 3×10^{11} cm^{-2} and a mobility of 3×10^5 cm^2/V sec at 4.2 K. Two parallel AuPd gates, each 52 nm wide and 0.5 μm long, were patterned 93 nm apart using electron-beam nanolithography, on a 5-μm-wide isolated 2D EG line [Fig. 1(b)]. Ohmic contacts were made to the three regions defined by both gates. Biasing the gates negatively with respect to the central region between them (called the base) depleted the 2D EG underneath the gates and prevented the free motion of the equilibrium electrons among the three regions [emitter (E), base (B), and collector (C)]. The potential barriers shown in Fig. 1(a) give an approximate guide to the potential shape for different gate voltages (which are about -0.5 V). The separation between the Fermi level, E_F, and the conduction band outside the base is 10.7 meV. In the base this separation can be substantially smaller, and the actual conductive width of the base (always smaller than the geometrical separation between the gates) was roughly estimated to be, for example, 70 nm when both barriers were 10 meV above the Fermi level [Fig. 1(a)]. Since this distance is similar to the average electron Fermi wavelength in the base, the base electrons are expected to be quasi-one-dimensional.

With no applied gate voltages, the measured resistances at 4.2 K among all three terminals (E, B, and C) were a few kilohms and constant with the applied terminal voltage. As the emitter- (or collector-) gate voltage, V_{GE} (or V_{GC}) was made negative with respect to the base (which was the reference in all our measurements), the emitter current, I_E, supplied by a source V_{EB} (or the collector current, I_C, supplied by a source V_{CB}) decreased. For gate voltage V_{GE} (or V_{GC}) < -0.4 V the resistance under the gate became very nonlinear and approached 10^8–10^9 Ω at low voltage (shown by I_E vs V_{EB} in Fig. 2). Simple WKB calculations of the tunneling currents through square barriers 50 nm wide and 20 meV high, resembling our barriers, resulted in similar tunneling resistances. The occurrence of tunneling through the barriers will be revisited and verified later in more detail. When only the emitter barrier was formed ($V_{GE} < -0.4$ V, $V_{GC}=0$), the emitter current I_E, which resulted from a negative V_{EB}, split into I_B and I_C in the ratio of the base and collector resistances of the 2D EG (note that $V_{CB}=0$ V). When the spectrometer barrier was also induced ($V_{GE} < -0.4$ V, $V_{GC} < -0.4$ V), the current in the collector remained practically zero (and $I_B=I_E$) until $|V_{EB}|$ exceeded a certain value (collector-current onset value). Thereafter it increased sharply. As seen in Fig. 2, the onset value increased as $|V_{GC}|$ increased and was similarly affected by an applied small V_{CB}. These

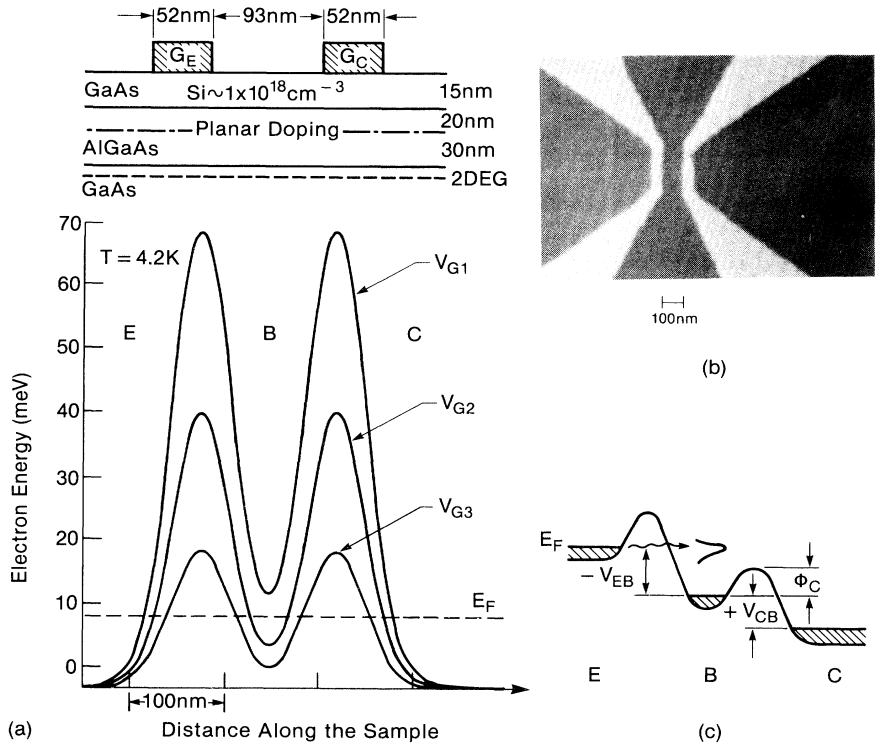

FIG. 1. (a) A cross-sectional cut showing the selectively doped structure and the gates on top. Underneath is plotted the potential shape in the lateral direction showing injector and spectrometer barriers. As V_G became more negative the potential barrier increased. (b) A scanning electron micrograph showing the gate configuration. (c) A schematic description of the potential distribution for a biased device, $V_{EB} < 0$ and $V_{CB} > 0$.

observations, which clearly resulted from changes in the spectrometer barrier height, Φ_C, demonstrate that the abrupt onset of I_C is due to energetic electrons that surmount the spectrometer barrier potential [see Fig. 1(c)]. Considering the small distance between injector and spectrometer barriers, a fraction of the electrons injected from the Fermi level in the emitter was expected to traverse the base ballistically, leading to collector-current onset at $eV_{EB} = \Phi_C$, where Φ_C is the collector barrier height. This allowed us to measure Φ_C, a result we can use to further verify the existence of ballistic transport and find the actual fraction of ballistic electrons arriving at the collector.

We have performed electron energy spectroscopy[1,4,5] by varying the spectrometer barrier height Φ_C with V_{CB}. The collected current is given by $I_C = A\int_{\Phi_c}^{\infty} en(E) \times v(E)dE$, where A is the area, $n(E)$ is the energy distribution of the electrons arriving at the spectrometer, and E and v are the energy and velocity associted with the electrons traversing normal to the gates. In a small enough energy range $v(E)$ is fairly constant, and the electron energy distribution can be described by $n(E) \propto dI_C/d\Phi_C$ for a constant injection energy, eV_{EB}. The same expression can be rewritten as $n(E) \propto (dI_C/deV_{CB})(deV_{CB}/\, d\Phi_C)$. Figure 3(a) (solid lines) shows a typical family of I_c vs V_{CB} characteristics for $V_{GE} = V_{GC} = -0.5$ V and different injection energies, all chosen to be higher than the unbiased spectrometer barrier height (for $V_{EB} = 0$ V, $I_C = 0$ in the range of interest). For $V_{CB} > 0$, the collector current increased only slowly as V_{CB} increased, suggesting that most of the hot electrons had energies higher than the unbiased potential barrier height. When the polarity of V_{CB} was reversed, leading to an increase in Φ_C, the collector current decreased slowly initially, followed subsequently by a sharp drop to zero over a range of a few mV. This behavior indicates that electrons with a narrow energy distribution were cut off by the spectrometer barrier. Before elaborating more on the shape of the energy distribution we would like to note that for injector barrier heights smaller than some 20 meV ($V_{GE} > -0.5$ V) the behavior was quite different, as shown for two lower injector barrier heights [dotted lines in Fig. 3(a)]. The collector currents became zero at the same negative V_{CB} (and thus the same Φ_C) for the three cases. This indicates that, even though the nature of the injection in each case may have been different, the highest energy of the injected and collected electrons was always determined by eV_{EB}. The absence of a "knee" observed for the lower injector barriers indicates that the injected distributions were broad, extending from the injection energy eV_{EB} and below, and were not the result of tunneling. It is quite possible that

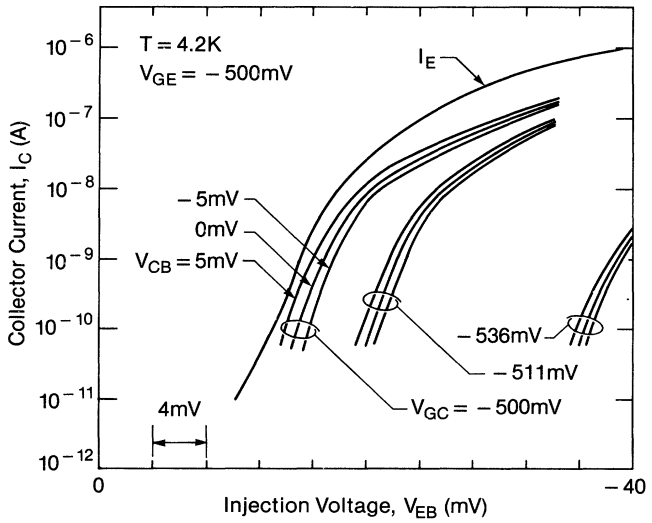

FIG. 2. The collector current I_C as a function of the injection voltage V_{EB} when the collector-gate voltage V_{GC} and the collector-base voltage V_{CB} serve as parameters. The current onset, indicative of the collector barrier height, is strongly influenced by both parameters. The injected current I_E is independent of the parameters.

when the injector barrier was low, the application of an injection voltage removed the barrier completely, or made it so narrow that the injected electron distributions were very broad.

To determine the collected energy distributions one has to change the energy scale from eV_{CB} to the corresponding height of the spectrometer barrier Φ_C, and multiply the dI_C/deV_{CB} curves by the $deV_{CB}/d\Phi_C$. The barrier heights $\Phi_C(V_{CB})$ and the factor $deV_{CB}/d\Phi_C$, summarized in Fig. 3(b), were found from collector-current onset measurements in a similar way to that described before. The energy distributions shown in Fig. 3(c) have a full width at half maximum of about 5 meV, which tended to increase as the injection energy increased [up to 10 meV for eV_{BE} = 30 mV (not shown)]. The peaks of the distributions shifted with the same energy as that of injection energy (except the lowest one which was obscured by the lower-energy tail), as expect-

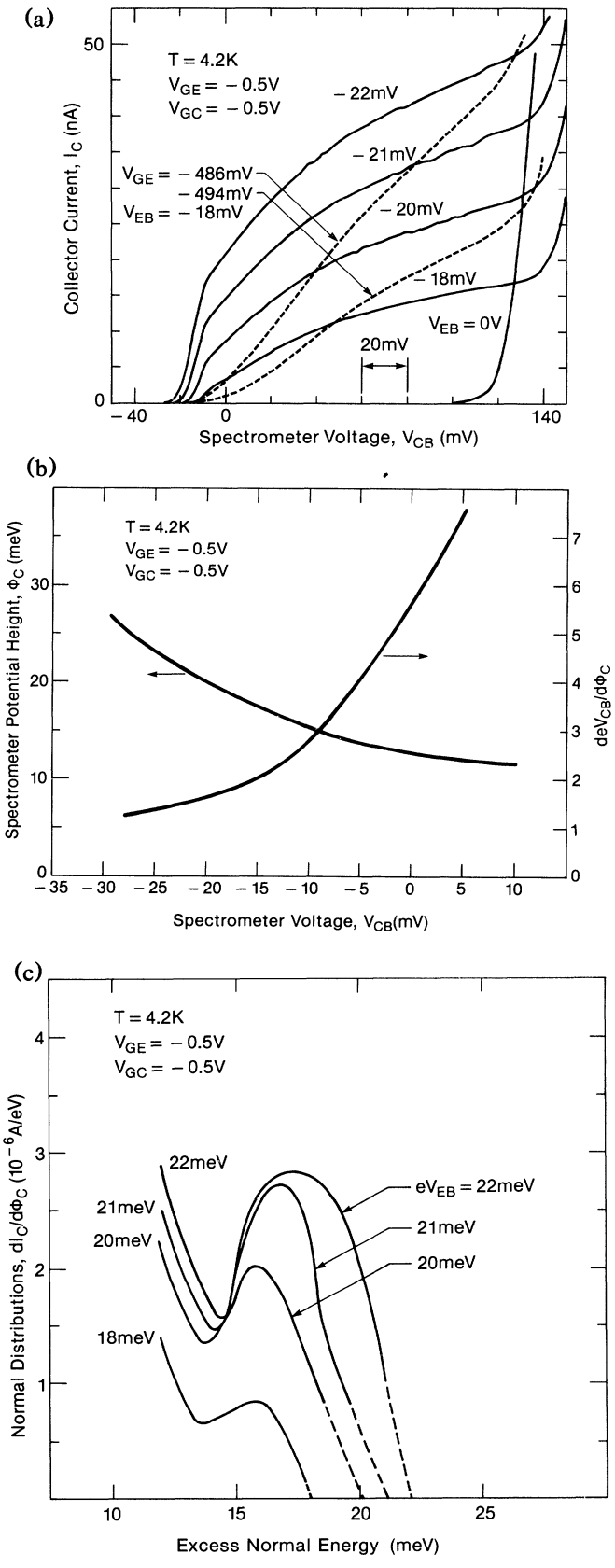

FIG. 3. (a) The family of the collector-current characteristics where I_E = 0, −20, −40, −60, −80 μA. Note the sharp rise in the current (for $V_{CB} \simeq -10$ mV) followed by a moderate rise indicative of a narrow ballistic distribution. The dotted lines are for lower injector barrier heights and for $eV_{EB} = -18$ mV, where the injected distributions were very broad. (b) The spectrometer barrier height determined by measuring the collector-current onsets, and the $deV_{CB}/d\Phi_C$ deduced from it. (c) The ballistic distributions for different injection energies as a function of excess normal energy above the Fermi level in the base. The peaks of the distributions follow rigidly the injection energy. At higher $|V_{CB}|$ leakage currents dominated.

ed in ballistic transport. The peak energies, which were lower by about 3–4 meV than the corresponding Fermi level in the emitter (noted by the crossing of the dotted lines with the energy axis), and the narrow distribution width ($\simeq$5 meV) were both expected for the normal energy distributions injected by 50-nm-wide, 20-meV-high tunnel barriers.[6] These results proved that tunneling was the injection mechanism in our induced barriers. At their lower-energy tails the distributions rise again, most probably due to lower-energy electrons that are excited from the Fermi sea in the base by scattered (nonballistic) electrons.[4] Even though small-angle elastic-scattering events cannot be excluded, the similarity of the results presented here with the results that confirmed ballistic transport in vertical structures,[1] as well as the narrow width of the electron distributions, strongly suggests that elastic scattering in our lateral structures was minimal.

The ballistic fraction, α, is defined as the ratio between the number of ballistic electrons collected (the ballistic current is I_C at $V_{CB}=0$ or the area under the distribution) and the total number of injected electrons (the injected current I_E). From Fig. 3(a) we find $I_C/I_E\simeq 0.25$ at $V_{CB}=0$, which is approximately the ballistic fraction collected. Since some of the injected current emerged from the periphery of the injector barrier (where the separation between them increases) and never surmounted the spectrometer barrier, the value 0.25 was not appropriate to use for the calculation of the ballistic mean free path (λ). To minimize the number of these "stray" electrons, different structures where the collector gate was 3 times longer (0.75 μm) than the emitter gate (0.25 μm) were made (base width 170 nm). Carrying out energy spectroscopy in these devices, ballistic fractions higher than 0.7 (Ref. 7) were measured. Using $\alpha=\exp(-d_B/\lambda)=0.7$, where d_B is the effective base width for the hot electrons, we find $\lambda\simeq 480$ nm. This lower limit on λ suggests that the mean free path of the hot electrons is on the same order as that of cold electrons. This might result in part from the relatively low density of electrons in the base and from size quantization effects in the quasi-one-dimensional base that may reduce the scattering cross sections.[8]

Since tunneling occurred into a quantized base, we have looked for, but did not observe, resonant tunneling effects in the injection currents.[9] Upon increasing the injection energy, but keeping $e|V_{EB}|<\Phi_C$, we had expected to see an enhancement in the injected current when the Fermi level in the emitter crossed a bound state in the base. To get a rough idea of the expected positions of the states, we modeled our double-barrier potential with a sine function, having a peak-to-peak value of 30 meV and a period of 140 nm. The solutions, which involved Mathieu functions,[10] predicted two states under the Fermi level (3 and 8.6 meV), and five states above (14, 19, 23.5, 27, and 29.5 meV). Since emitter currents could be measured only for $V_{EB}<-(10\text{–}15)$ mV, only the highest two states (near the continuum) could in principle have been observed. Because of the finite width of the distribution ($\simeq$5 meV) it would be difficult to resolve these states from the continuum. In cases of lower barrier heights the energy separation between the states was expected to be even smaller and their energy width wider, making observation difficult.

In summary, we have seen for the first time, lateral tunneling through narrow potential barriers induced by thin gates, and ballistic hot-electron transport with a long mean free path, in a two-dimensional electron-gas (2D EG) channel. Via the utilization of an energy spectroscopy technique, narrow electron distribution injected by a tunneling barrier were detected, establishing directly ballistic transport and tunneling injection. We estimate a ballistic mean free path for hot electrons of about 0.48 μm.

We would like to thank L. Osterling for his help with the molecular-beam-epitaxy growth, M. Weckwerth for his help with processing, P. M. Soloman and F. Stern for useful discussions, and T. W. Hickmott, C. J. Kircher, and S. Washburn, for their comments on the manuscript. One of us (A.P.) would like to thank R. B. Laibowitch for his continuous support. The work was partly supported by the U.S. Defense Advanced Research Projects Agency and administered by ONR, Contract No. N00014-87-C-0709.

---

[a]Permanent address: Department of Engineering, Cambridge University, Cambridge, England.

[1]M. Heiblum, M. I. Nathan, D. C. Thomas, and C. M. Knoedler, Phys. Rev. Lett. **55**, 2200 (1985).

[2]D. A. Wharam, T. J. Thornton, R. Newbury, M. Pepper, H. Ahmed, J. E. F. Frost, D. J. Hasko, D. C. Peacock, D. A. Ritchie, and G. A. Jones, J. Phys. C **21**, L209 (1988).

[3]B. J. van Wees, H. van Houten, C. W. J. Beenakker, J. G. Williamson, L. P. Kouwenhoven, D. van der Marel, and C. T. Foxon, Phys. Rev. Lett. **60**, 848 (1988).

[4]M. Heiblum, K. Seo, H. P. Meier, and T. W. Hickmott, Phys. Rev. Lett. **60**, 828 (1988).

[5]D. J. Dimaria, M. V. Fischetti, J. Batey, L. Dori, E. Tierney, and J. W. Stasiak, Phys. Rev. Lett. **57**, 313 (1986).

[6]M. Heiblum, D. Galbi, and M. Weckwerth, Phys. Rev. Lett. **62**, 1057 (1989); K. Seo (private communication).

[7]When emitter and collector were reversed in the asymmetric device, the ballistic fractions decreased approximately by the ratio between the gate lengths (1:3); another indication of the straight trajectories of the electrons in their ballistic motion. This work will be published later.

[8]D. C. Herbert (private communication).

[9]M. Heiblum, M. V. Fischetti, W. P. Dumke, D. J. Frank, I. M. Anderson, C. M. Knoedler, and L. Osterling, Phys. Rev. Lett. **58**, 816 (1987).

[10]*National Bureau of Standards, Tables Relating to Mathieu Functions* (Columbia Univ. Press, New York, 1951).

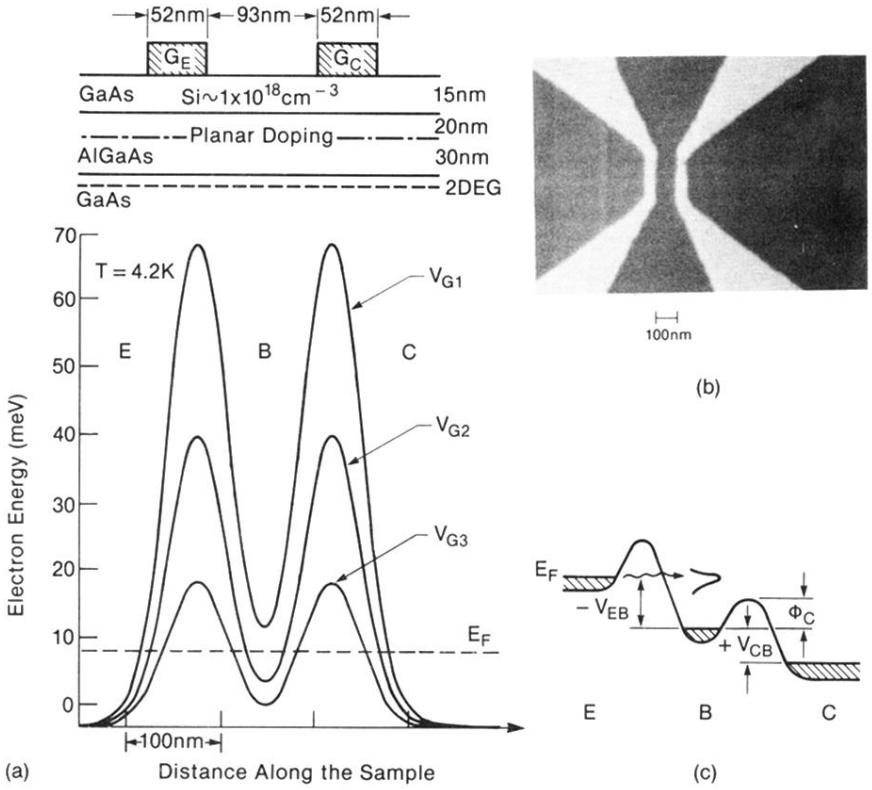

FIG. 1. (a) A cross-sectional cut showing the selectively doped structure and the gates on top. Underneath is plotted the potential shape in the lateral direction showing injector and spectrometer barriers. As V_G became more negative the potential barrier increased. (b) A scanning electron micrograph showing the gate configuration. (c) A schematic description of the potential distribution for a biased device, $V_{EB} < 0$ and $V_{CB} > 0$.